Probing Hg evasion from surface waters of two Chinese hyper/meso-eutrophic reservoirs

Xuewu Fu [a], Xinbin Feng [a,*], Qi Wan [a], Bo Meng [a,b], Haiyu Yan [a], Yanna Guo [a]

[a] State Key Laboratory of Environmental Geochemistry, Institute of Geochemistry, Chinese Academy of Sciences, Guiyang 550002, PR China
[b] Graduate University of the Chinese Academy of Sciences, Beijing 100049, PR China

ARTICLE INFO

ABSTRACT

Measurements of water/air exchange flux of gaseous elemental mercury (GEM) were conducted in a hyper-eutrophic reservoir and a meso-eutrophic reservoir in southwest China in both warm and cold seasons by using a dynamic flux chamber (DFC) method coupled with an automatic gaseous Hg analyzer. Both strong diurnal and seasonal variations of GEM fluxes were observed. The diurnal cycle of the GEM flux was more pronounced during sunny days compared to cloudy and rainy days, which highlights the effect of solar intensity on the GEM flux. GEM fluxes in warm seasons were considerably higher (2.5 to 4.1 times higher) than in cold seasons, which was attributed to the combined factors including meteorological factors, water quality parameters and water Hg concentrations. Clear variation in GEM fluxes was observed between the two reservoirs. Mean GEM fluxes in the hyper-eutrophic reservoir (WJD) ($3.2–20.1$ ng m^{-2} h^{-1}) were significantly higher than those in the meso-eutrophic reservoir (SFY) ($0.6–4.4$ ng m^{-2} h^{-1}). Evasion of Hg played a distinct role in the mass balance of Hg in the two reservoirs. In WJD, evasion was the second most important mechanism for Hg losses from the reservoir (17.5% of the total losses); whereas in SFY, loss of Hg via volatilization constituted an extremely little portion to the total losses of Hg (0.8%).

© 2010 Elsevier B.V. All rights reserved.

1. Introduction

Dynamics of mercury (Hg) in aquatic ecosystem is of particular concern because Hg delivered to watersheds can be converted to monomethylmercury (MeHg), a highly toxic, persistent and bioaccumulative species that poses a serious threat to human health and wildlife by consuming fish. Exchange of Hg between aquatic environments and atmosphere plays a crucial role in the biogeochemical transformation and cycling of Hg in aquatic ecosystems and atmospheric Hg budget. First, for most remote aquatic environments, atmospheric deposition is the dominant source (Jeremiason et al., 2009; Selvendiran et al., 2009). On the other hand, evasion of Hg from water driven by formation of Hg^0 (DGM) by photochemical and microbial reduction could reduce the Hg burden in the water column which would have an inverse effect on the MeHg production and bioaccumulation (Mason et al., 1999). Also, evasion of Hg from water bodies is identified as one important source of atmospheric Hg (Mason and Sheu, 2002; Strode et al., 2007).

China is one of the largest anthropogenic sources to the global atmospheric Hg budget. This results in elevated deposition flux in China (Guo et al., 2008a; Wang et al., 2008b), which in turn increases the Hg burden in aquatic environments. It is well known that previously deposited Hg is likely reemitted to the atmosphere. It is therefore expected that aquatic environments in China might have higher Hg emission flux compared to other regions world-wide (Feng et al., 2004a, 2008a). Besides, aquatic environments in China are generally exposed to largest discharges of untreated municipal sewage, agricultural runoff, and aquaculture wastewater, which could result in a series of negative ecological impacts including eutrophication and water deterioration (Qin et al., 2006; Liu et al., 2009). Eutrophication may play an important role in Hg transport and immobilization (Coelho et al., 2005). It is characterized by frequently recurring algal blooms which may result in an increased microbial activity and changes in redox potential, pH, and concentrations of Fe and Mn compounds (Eggleton and Thomas, 2004), and many studies have revealed its impacts on the biogeochemical cycling of Hg in aquatic environments and food chain (Radway et al., 2001; Pickhardt et al., 2002; He et al., 2008). However, the impact of eutrophication on the water/air Hg flux is still limited and deserves further studies.

Reservoirs have been increasingly created in China to fulfill the rapidly increased demand for energy needs. It is estimated that the area of reservoirs in China reaches 2.1×10^4 km^2, which constitutes about 15% of the total inland water area in China. Aquaculture activities are extremely developed in most reservoirs of China. This has resulted in a series of negative ecological impacts to aquatic environments including elevation of total organic matter content, eutrophication or algae bloom (Cao et al., 2007) due to the discharges of wastewater and fish feed with a high concentration of nitrogen and phosphorus nutrients. This may have an important impact on water/air exchange of Hg. Hence, it will be
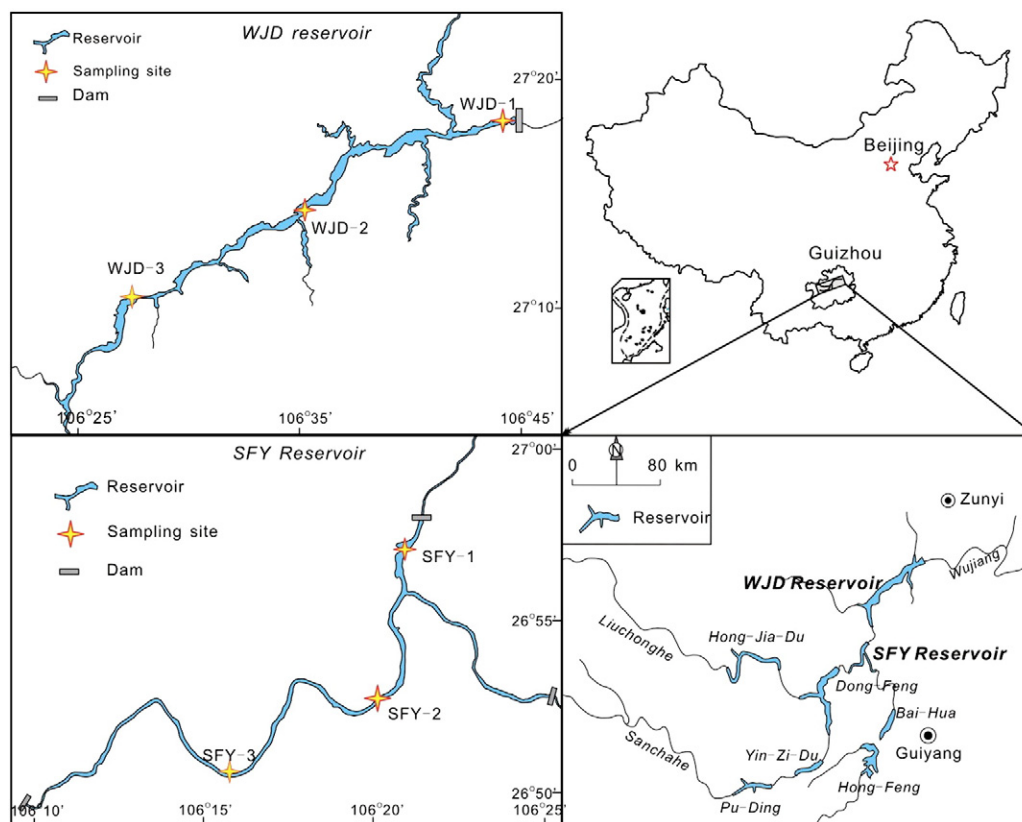

Fig. 1. Map showing the two studied reservoirs and the experimentation sites.

of importance to make proper quantification of evasion of Hg from reservoirs and evaluate the Hg cycling in these aquatic environments of China.

In this study, we selected two distinct channel-type reservoirs located on the Wujiang River, which is a branch of Yangtze River, in Guizhou province, southwest China, and made comprehensive measurements with regard to the spatial and seasonal variations of water/air Hg exchange fluxes. The main purposes of this study were to: (1) better understand the spatial and seasonal variations of water/air Hg flux and the processes influencing the flux in channel-type reservoirs; (2) evaluate the impact of eutrophication on the water/air Hg flux; and (3) evaluate contributions of Hg volatilization to the mass balance of Hg in reservoirs.

2. Experimental

2.1. Site locations

Two reservoirs, Wujiangdu (WJD) and Suofengying (SFY), were selected for measuring exchange fluxes of Hg between water and atmosphere, which are located on the Wujiang River, one of biggest branches of upper Yangtze River (Fig. 1). The two reservoirs are situated on the Yunnan–Guizhou Plateau with the altitude of 700–900 m above sea level. Climate in the study area belongs to the

subtropical moist and warm climate region, with distinct rainy (May to October) and dry (November to April) seasons. The annual average temperatures for WJD and SFY were in the range of 14–16 °C, and annual precipitation depths were in the range of 700–1200 mm.

The two studied reservoirs were quite distinct from each other, and the basic information of these two reservoirs is given in Table 1. WJD is the oldest reservoir in Wujiang River, whereas SFY is the newest reservoir. WJD has much bigger storage capacity and water area compared to SFY. Furthermore, cage aquaculture activities are very prevalent in the WJD reservoir, and it is reported that the area of cage reached 37,200 m^2 in 2001 and increased significantly in recent years. This has resulted in a series of negative ecological impacts (e.g. eutrophication, water quality deterioration) in this reservoir (Yu, 2008; Wang et al., 2009). On the other hand, there are no cage aquaculture activities in the SFY reservoir.

For each of the reservoir, three sampling sites were selected to study the spatial distribution of Hg fluxes, which were located near the dam, middle and upper reach of the reservoirs, respectively (Fig. 1). Moreover, measurements were conducted in different seasons to study the temporal variations of Hg flux. The sampling campaigns in warm and cold seasons for WJD were carried out from 8 to 14 May in 2006 and from 31 Jan to 6 Feb in 2007, respectively, while the sampling campaigns for SFY were conducted from 13 to19 Oct 2006 and from 21 to 27 Jan 2007, respectively.

Table 1
Statistical summary showing features of the two reservoirs in this study.

	Operation time	Normal storage capacity (m^3)	Immersed area (m^2)	Maximum depth (m)	Annual discharge (m^3)	Water residence time (day)	Vertical stratification	Mean water flow (m s^{-1})
WJD	1979	13.5×10^8	47.8×10^6	120	158×10^8	~30	Yes	0.06
SFY	2005	0.67×10^8	5.7×10^6	90	125×10^8	~2	No	0.1

2.2. Sampling techniques and analysis

Exchange fluxes of Hg between water and atmosphere were measured by using a dynamic flux chamber (DFC) made of Quartz glass coupled with automated Hg vapor analyzer (Tekran 2537A) (Feng et al., 2004a, 2008a). Water/air Hg flux was obtained via measuring the difference in atmospheric Hg concentrations inside and outside the flux chamber and exchange flux of air mass in the chamber. Water/air exchange flux of Hg was estimated using the following equation:

$$F = (C_o - C_i) \times Q / A \qquad (1)$$

where F is flux in ng m^{-2} h^{-1}; C_o and C_i are Hg concentrations of the outlet and inlet air stream (ng m^{-3}); Q is the flushing flow rate through the chamber (0.9 m^3 h^{-1}); and A is the enclosed water area (0.12 m^2). In this study, it is speculated that the measured Hg concentration was dominated by GEM, and this could be caused by many factors as those described below. First, PHg was removed using a 45 mm diameter Teflon filter (pore size 0.2 μm). Moreover, RGM in ambient air above water surface was likely removed when passing the sampling tube, which should have very high humidity in it and was installed with a soda lime before entering the Tekran instrument. Therefore, the atmospheric Hg measured herein was referred to as GEM. Alternate measurements of GEM concentrations in air from the inlet to the outlet of the chamber every 10 min were achieved by using a magnetic 3-way valve (Tekran 1110). Previous studies by Zhang et al. (2002) and Lindberg et al. (2002) demonstrated that soil Hg fluxes measured by DFC operations strongly depend on the flushing flow rates used, and high flushing flow rates (e.g. ~0.9–2.4 m^3 h^{-1} for DFCs of common design) are adopted. Although no reports showed that flushing flow rates affect Hg flux from water surface, we used a high flushing flow rate of 15 L min^{-1} to prevent the possibility of underestimating Hg flux at a low flushing flow rate (Feng et al., 2008a). The data quality of Tekran Model 2537A was guaranteed via periodic internal recalibration with a 25 h interval. Blanks of the chamber were measured with an ultra clean quartz glass plate and fell in the range of 0.01–0.12 ng m^{-2} h^{-1}. The blanks were small and we did not make blank correction for measured fluxes.

Total mercury (THg), reactive mercury (RHg) and dissolved mercury (DHg) concentrations in surface water at each of the sampling site were determined. Water samples were collected by hand using 100-ml borosilicate glass bottles at a depth of 10–30 cm below the water surface. To ensure clean operation, polyethylene gloves were used throughout the sampling. THg and DHg were analyzed by BrCl oxidation followed by SnCl$_2$ reduction, and dual amalgamation combined with CVAFS detection (US EPA, 1999), while RHg was analyzed by direct SnCl$_2$ reduction followed by dual amalgamation combined with CVAFS detection. DOC content in water was measured using a high-temperature combustion method (Cosovic et al., 2000). TSS was measured by collecting and weighing suspended particles from a measured volume of the water sample (1.5 L) with Teflon filter (Minipore, 0.45 μm). A portable weather station (Puhui, Wuhan, China) installed on the bank of the reservoir and 2 m above surface ground (within 50 m from the flux sampling site) was used to collect environmental parameters including solar radiation, air temperature, water temperature, wind direction, wind speed, and air relative humidity with a 5 min time resolution which matched the 5 min sampling interval of Tekran 2537A.

3. Result and discussion

3.1. Hg concentrations and water quality parameters in surface water

Statistical summary of Hg concentrations and water quality parameters in surface water are shown in Table 2. In general, WJD

Table 2
Statistical summary of water/air Hg fluxes, atmospheric GEM concentrations, meteorological and water quality parameters during the whole sampling period.

Site	Season	GEM flux (ng m^{-2} h^{-1}) Mean±std	Range	N Emission (deposition)	GEM conc. (ng m^{-3}) Mean±std	Range	Solar radiation (w m^{-2})	Air temp (°C)	Wind speed (m s^{-1})	Air humidity (%)	THg (ng L^{-1})	RHg (ng L^{-1})	DOC (mg L^{-1})	TSS (mg L^{-1})
WJD-1	Warm	20.1±10.4	3.5–67.2	140 (0)	7.5±2.1	3.8–13.2	63±123	21.0±2.5	3.6±0.6	86.8±13.8	2.68	0.36	2.62	1.60
	Cold	6.2±9.8	−7.8–45.3	84 (18)	10.3±5.4	6.4–38.2		11.0±2.3	1.6±1.7	79.7±14.5	1.82	0.26	0.68	2.17
WJD-2	Warm	14.1±5.4	5.5–29.3	130 (0)	6.5±2.2	3.8–12.2	103±175	18.6±2.0	3.9±0.9	83.3±9.1	2.13	0.29	3.49	3.13
	Cold	4.7±7.1	−3.4–37.5	121 (20)	9.7±2.8	4.2–18.6		12.0±3.3	0.9±1.3	75.1±14.7	1.25	0.19	0.67	0.64
WJD-3	Warm	9.9±4.2	1.4–26.4	146 (0)	3.7±0.7	2.0–5.5	72±154	18.6±2.0	3.9±0.9	83.2±9.1	2.04	0.37	3.07	2.67
	Cold	3.2±4.6	−11.2–18.0	100 (19)	8.4±2.4	5.0–16.1	54±93	14±3.5	0.2±0.5	74.9±17.7	1.28	0.26	0.65	1.91
SFY-1	Warm	4.1±5.5	−4.0–27.4	111 (36)	15.9±3.5	10.1–26.5	30±74	21.9±1.3	0.3±0.6	86±8	1.40	0.40	0.72	0.92
	Cold	1.0±2.6	−6.4–11.6	87 (49)	7.0±1.8	4.7–17.6	88±187	6.4±1.2		72±6	1.10	0.12	0.89	1.23
SFY-2	Warm	1.5±3.1	−6.7–12.9	89 (25)	7.5±2.8	2.9–15.8	41±86	23.4±3.5	0.1±0.3	90±15	1.35	0.34	0.56	0.46
	Cold	0.6±2.5	−3.8–9.0	69 (56)	8.4±1.6	5.4–15.9	84±164	8.8±1.1		65±8	0.87	0.09	0.58	0.84
SFY-3	Warm	4.4±5.1	−2.3–23.9	114 (8)	6.9±1.6	3.4–11.3	15±33	22.9±2.8	0.1±0.2	88±14	2.12	0.22	0.66	0.66
	Cold	1.3±2.4	−3.0–10.5	49 (22)	9.3±1.6	5.1–12.5		9.2±1.7		76±11	1.24	0.12	0.50	1.37

showed relatively higher THg (mean: 1.87 ng L^{-1}), and RHg (mean: 0.29 ng L^{-1}) concentrations compared to SFY (mean THg concentration: 1.35 ng L^{-1}, mean RHg concentration: 0.22 ng L^{-1}). In WJD, THg concentrations decreased with the distance from the dam, while this trend was not observed in SFY of which the site in the upper reach showed the highest THg concentrations. Consistent seasonal variations with elevated THg and RHg concentration in warm seasons were observed in both reservoirs (Table 2).

Hg concentrations in WJD and SFY were considerably lower compared to other aquatic environments in Guizhou province, southwest China. For example, Feng et al. (2004a) reported that THg and RHg concentrations in the Baihua reservoir were in the ranges of 12.1–42.6 and 1.8–4.6 ng L^{-1}, respectively. Additionally, Hongfeng Lake in Guizhou province also showed much higher THg and RHg concentrations (He et al., 2008). The lower levels of Hg in the study area may be due to the fact that the watersheds of both reservoirs are naturally preserved and a little amount of municipal sewage is discharged to this area, whereas Baihua and Hongfeng lakes were heavily polluted by municipal sewage discharges and atmospheric Hg deposition driven from industrial and urban areas nearby (He et al., 2008; Yan et al., 2009). On the other hand, water Hg concentrations in this study were comparable to those of pristine water from Europe and North America which were generally less than 2 ng L^{-1} (Schroeder et al., 2005; Zhang et al., 2006; Muresan et al., 2008a,b).

3.2. GEM concentrations in ambient air over water surface

GEM concentrations in ambient air above water surface are shown in Fig. 2. In general, GEM concentrations were characterized by significant variations throughout the sampling campaign, and episodes with highly elevated GEM concentrations (e.g. GEM concentrations measured during the nighttime of Oct 13 and later afternoon of Oct 14 in 2006 at SFY-1) were probably due to encounters of air masses originated from industrial and urban areas. Mean GEM concentrations in the study area ranged from 3.73 to 15.9 ng m^{-3} (Table 2). Our results are consistent with GEM concentrations reported in Baihua (4.6–9.96 ng m^{-3}, Feng et al., 2004a) and Hongfeng reservoirs (5.1–9.76 ng m^{-3}, Feng et al., 2008a). Obviously, GEM concentrations in this region were highly elevated compared to the results observed in North America and Europe (1.0–2.6 ng m^{-3}, Gårdfeldt et al., 2001; Zhang et al., 2006; O'Driscoll et al., 2007). We attributed it to the high anthropogenic emissions and natural emission from Hg enriched soil in Guizhou province (Feng and Qiu, 2008b), which is the second biggest atmospheric Hg source region in China (Wu et al., 2007).

Aside from the site located near the Dam of SFY, GEM concentrations observed in the cold season sampling campaigns were elevated compared to those in the warm season (p<0.01, Table 2). Fig. 3 shows the correlation analysis between atmospheric GEM concentrations and solar radiation (since solar radiation was not measured in the WJD reservoir in the warm season, air temperature is used in the correlation analysis as air temperature could be a proxy of solar radiation), which is generally regarded as a key factor regulating soil and water Hg emission fluxes (e.g. Poissant and Casimir, 1998; Boudala et al., 2000; Gårdfeldt et al., 2001). In general, GEM concentrations in WJD exhibited a positive linear relationship with air temperature and solar radiation; whereas GEM concentrations in the SFY reservoir showed a negative and a very weak linear relationship with solar radiation, respectively. This indicates that natural emissions of Hg in the WJD reservoir were an important source of atmospheric GEM in both warm and cold seasons; whereas natural sources in SFY played a limited role in influencing atmospheric GEM concentrations. However, as natural emissions of Hg generally decrease in the cold season due to the lower air temperature and solar radiation, the elevated cold season GEM concentrations might be likely attributed to increased anthropogenic Hg emissions and

decreased atmospheric scavenge processes (Feng et al., 2004b; Fu et al., 2009, 2010). GEM concentrations varied significantly among sites, and sites close to the dam which were generally related to population centers and industrial areas showed higher levels compared to other sites. It highlights that local emissions sources contributed significantly to GEM levels.

3.3. Diurnal and seasonal variation of GEM flux

A consistent diurnal distribution pattern with elevated fluxes in the daytime and low fluxes in the night was observed at all the sites in both warm and cold seasons (Fig. 2). This pattern was more pronounced during sunny days compared to cloudy and rainy days. GEM fluxes generally showed highest values at noon which were closely related to the peaks of solar radiation, and correlation analysis shows that GEM fluxes were strongly correlated with solar radiation (Table 3). For other meteorological parameters, there was no consistent relationship with GEM fluxes. GEM concentrations exhibited distinct relationships with GEM fluxes in WJD and SFY reservoirs. In WJD, GEM concentrations were often positively linked to GEM fluxes; whereas in SFY, GEM concentrations were often negatively correlated with GEM fluxes. This suggests that evasion of Hg from water in WJD constituted an important fraction of the source of atmospheric GEM because of high evasion GEM fluxes (Section 3.3). However, it seems that relatively higher GEM concentrations in SFY (1.48 ng m^{-3} higher in mean concentration compared to WJD) had an inverse effect on GEM fluxes, or they were controlled by different mechanisms.

Seasonal variation in the GEM flux was statistically significant ($p_{WJD}<0.01$, $p_{SFY}=0.01$) in the study area. The magnitudes of GEM fluxes in warm season were 2.5–4.1 times higher compared to the fluxes in the cold season (Table 2). Besides, episodes with deposition fluxes significantly increased in the cold season compared to the warm season (Table 2). Generally, seasonal variation in the GEM flux was suggested to be related to the seasonal variations of environmental factors (Schroeder et al., 2005). Here, it is speculated that the seasonal variability in GEM fluxes reflects the combined effects of environmental parameters, water quality parameters and Hg levels. Firstly, increased solar radiation, air temperature, wind speed, and lower atmospheric GEM concentrations in warm season probably drove an increase in the GEM flux (Boudala et al., 2000; Gårdfeldt et al., 2001; Wang et al., 2006). Secondly, it is speculated that increased DOC concentrations in water in the warm season also promoted GEM emission flux. Peters et al. (2007) suggested that large increase (2–14 mg L^{-1}) in DOC could promote the production of DGM which could drive an increase in flux. DOC concentrations in WJD in the warm season were elevated compared to the cold season (Table 2), which probably enhanced the evasion of Hg. Finally, seasonal variation in THg concentrations of water may also be responsible to the seasonal variation of the GEM flux. Previous studies by Schroeder et al. (2005) and Wollenberg and Peters (2009) found a positive relationship between GEM fluxes and THg concentrations in aquatic environments, suggesting that increased Hg concentrations in water could result in elevated fluxes. In this work, elevated THg and RHg concentrations in warm season were observed from all the sampling sites, which was probably due to the great loading of Hg. The higher loading of Hg in the warm season might drive an increase in Hg reemissions.

3.4. Comparisons of GEM fluxes between the two reservoirs and other aquatic environments

In general, net emissions of GEM were observed at all the sampling sites, indicating that water bodies in the study areas presented as net GEM sources to the atmosphere. The average GEM fluxes at the three sites of WJD in warm season and cold season were in the ranges of 9.9 to 20.1 and 3.2–6.2 ng m^{-2} h^{-1}, respectively; whereas SFY showed much
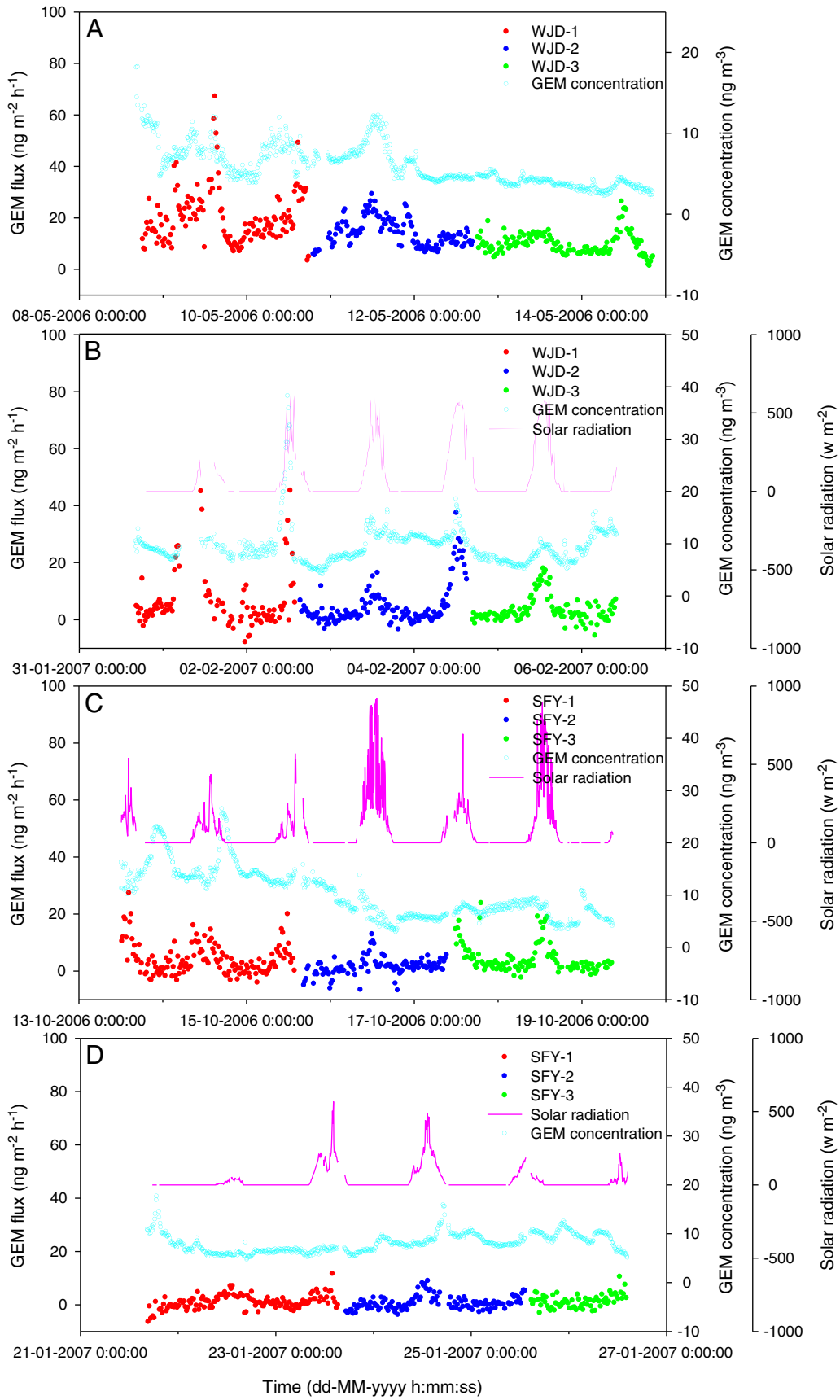
Fig. 2. Water/air GEM fluxes, GEM concentrations in ambient air above water surface and solar radiation in A) WJD in the warm season, (B) WJD in the cold season, (C) SFY in the warm season; and (D) SFY in the cold season.
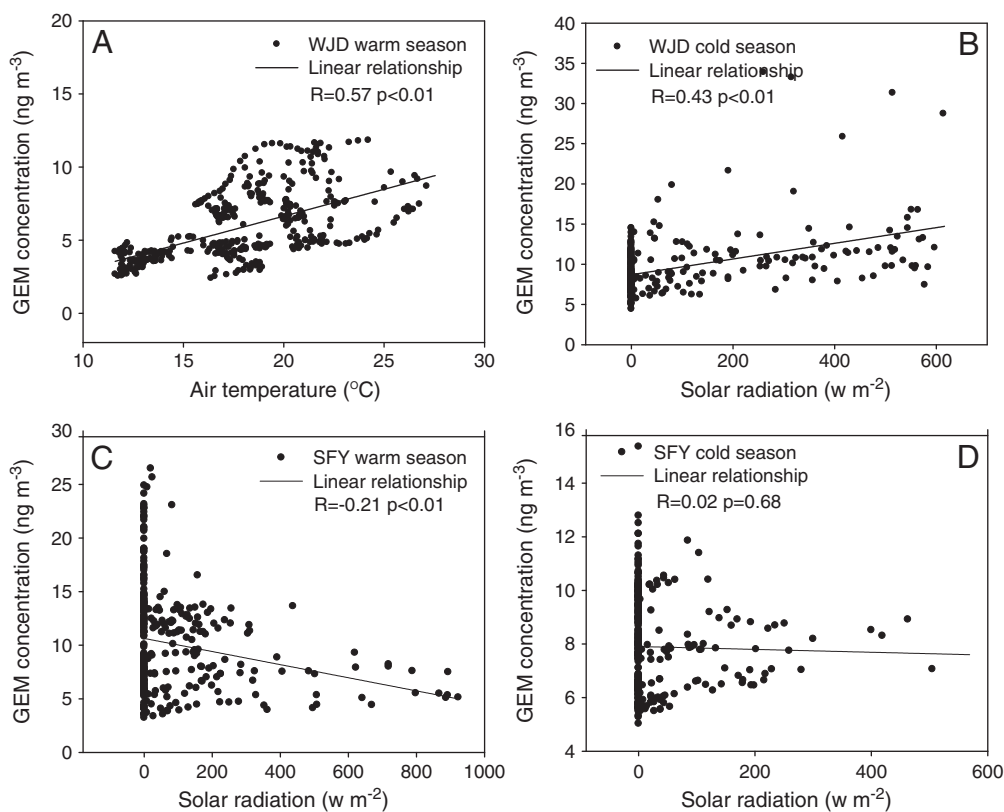
Fig. 3. Correlation analysis between GEM concentrations and air temperature and solar radiation in A) WJD reservoir in the warm season; B) WJD reservoir in the cold season; C) SFY reservoir in the warm season; and D) SFY reservoirs in the cold season.

lower GEM fluxes compared to WJD, with the ranges of 1.5–4.4 and 0.6–1.3 ng m^{-2} h^{-1} in warm season and cold season, respectively. Totally, GEM fluxes in WJD were higher or comparable to those reported from Baihua (3.8–7.4 ng m^{-2} h^{-1}, Feng et al., 2004a) and Hongfeng reservoirs (1.8–6.5 ng m^{-2} h^{-1}, Feng et al., 2008a), which were Hg polluted reservoirs; whereas GEM fluxes in SFY were lower than those two reservoirs. On the other hand, GEM fluxes in WJD and SFY were much higher than those reported from North America (Poissant and Casimir, 1998; Boudala et al., 2000; Schroeder et al., 2005; Zhang et al., 2006; Muresan et al., 2007, 2008b), but comparable to the results observed from Sweden (Xiao et al., 1991; Lindberg et al., 1995).

Significant variation in GEM fluxes was observed from the two reservoirs (p = 0.02). The mean GEM flux in WJD was about 4.5 folds higher compared to SFY. Fig. 4 shows the comparison of GEM fluxes between WJD and SFY in the warm season. Both daytime and night mean GEM fluxes in WJD were significantly elevated compared to SFY

(p in the daytime: 0.04; p in the nighttime: 0.008). Interestingly, WJD GEM flux/SFY GEM flux ratios during the night (ranged from 5.3 to 23, difference T test p<0.01) were much higher compared to those in the daytime (range from 1.6 to 8.2, difference T test p = 0.045). The significant difference in GEM fluxes between WJD and SFY could be the results of combined factors. First of all, the SFY reservoir has a much shorter water residence time compared to WJD. This probably decreased the chemical and physical reactions of Hg in water body and limited the formation of DGM. Also, the short water residence time in SFY also accelerated the vertical water exchange, and this might decrease the surface water DGM concentrations because of the exchange with low DGM concentration deep waters. Beside, we suppose that eutrophication played an important role in regulating GEM fluxes in these two reservoirs.

The WJD reservoir, which is immediately downstream of the SFY reservoir, has a similar geological background, soil type, climate

Table 3
Correlation analysis results (R and p values) between Hg flux and atmospheric GEM concentration and environmental parameters.

Season	Site	Solar radiation	Air temperature	Wind speed	Air humidity	GEM concentration
Warm season	WJD-1	–	0.14[*]	0.22[**]	−0.13	0.21[**]
	WJD-2	–	0.34[**]	0.60[**]	−0.09	0.68[**]
	WJD-3	–	0.12	0.06	−0.12	0.41[**]
Cold season	WJD-1	0.54[**]	0.16	−0.12	−0.10	0.45[**]
	WJD-2	0.84[**]	0.54[**]	−0.01	−0.39[**]	0.52[**]
	WJD-3	0.84[**]	0.27[**]	0.23[*]	−0.35[**]	0.03
Warm season	SFY-1	0.76[**]	0.44[*]	–	−0.41[**]	−0.38[**]
	SFY-2	0.50[**]	0.36[**]	–	−0.36[**]	−0.37[**]
	SFY-3	0.72[**]	0.57[**]	–	−0.56[**]	0.05
Cold season	SFY-1	0.48[**]	0.08	0.08	−0.01	−0.43[**]
	SFY-2	0.73[**]	0.29[**]	0.22[*]	−0.20[*]	0.20[*]
	SFY-3	0.57[**]	0.01	–	0.18	−0.39[**]

[*] Correlation is significant at level of p<0.05.
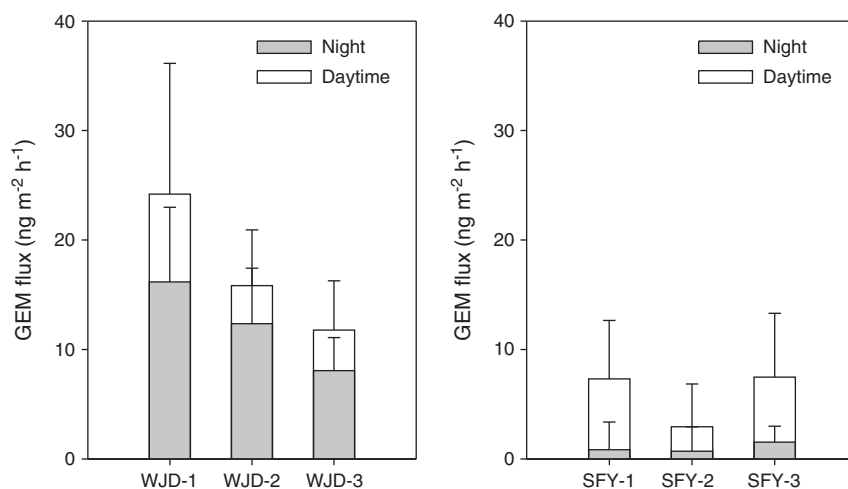[**] Correlation is significant at level of p<0.01.

Fig. 4. Comparisons of GEM fluxes between WJD and SFY reservoirs in warm season.

conditions and atmospheric Hg deposition as the SFY reservoir. However, GEM fluxes in WJD were significantly elevated (~4.5 folds higher) compared to SFY. It is speculated that the elevated GEM fluxes in WJD are likely attributed to the water eutrophication induced by aquaculture activities. Cage aquaculture activities have been operated since 1999 and increased significantly in recent years in WJD. Previous studies suggested that the annual mean fish feed used for aquiculture was about 10,000 tons and about 15–40% of which was lost to the water body (Sun et al., 2005). This has caused serious impacts on the water quality in the WJD reservoir. Yu (2008) reported that average contents of TN, TP and ChlorophyII in WJD were 8.46 mg L^{-1}, 0.469 mg L^{-1} and 8.99 μg L^{-1}, respectively; which were much higher compared to the SFY reservoir (TN: 7.57 mg L^{-1}, TP<detection limit (0.001 mg L^{-1}), Chlor-ophyII = 1.34 μg L^{-1}). Also, Wang et al. (2009) reported that the mean TP content (0.356 μg L^{-1}) in WJD was more than ten times higher compared to SFY. These results suggested that WJD is hyper-eutrophic and SFY is meso-eutrophic (Wang et al., 2008a,b, 2009; Yu, 2008).

There are several possible mechanisms for the hyper-eutrophic WJD reservoir exhibiting elevated GEM fluxes. First of all, the eutrophication in WJD was generally accompanied by elevated water THg concentrations (Table 2), which might result from discharges of fish feed and domestic sewage. As shown in Fig. 5A, GEM fluxes in WJD and SFY are both linearly correlated with water THg concentrations, respectively. This is consistent with the result reported by Schroeder et al. (2005) which also showed the positive

relationship between Hg fluxes and THg concentrations in water for the aquatic systems in Quebec and Nova Scotia, Canada. The elevated THg concentrations in WJD probably increased the available Hg concentrations for reduction, which in turn increased the GEM fluxes from water.

Secondly, many studies suggested that Hg reduction in water environment is triggered by DOC through its photoexcitation, and increasing emission flux of Hg as a function of DOC concentrations has been observed from both laboratory experiments and fresh aquatic systems (e.g. Tseng et al., 2004; Garcia et al., 2006; Peters et al., 2007). During the warm sampling campaign in the WJD reservoir, DOC concentrations were about 2.5 mg L^{-1} higher compared to other campaigns (Fig. 5B), owing to the enhanced fish farming. Accordingly, GEM fluxes in the warm season in WJD showed a clear increase compared to other campaigns. During the cold sampling campaign in the WJD reservoir, GEM fluxes were higher compared to those observed in the SFY reservoir, even through DOC and THg concentra-tions were comparable among these sites (Fig. 5B). This is likely attributed to the high solar intensity in WJD, which was higher or comparable compared to SFY. On the other hand, Amyot et al. (1997) suggested that high DOC concentration in fresh water systems tends to complex Hg(II) and reduce light penetration, which could reduce the production of DGM and in turn decrease water GEM evasion fluxes. But Tseng et al. (2004) suggested that Hg complexes with DOC were also photoreducible and contributed to production of DGM.
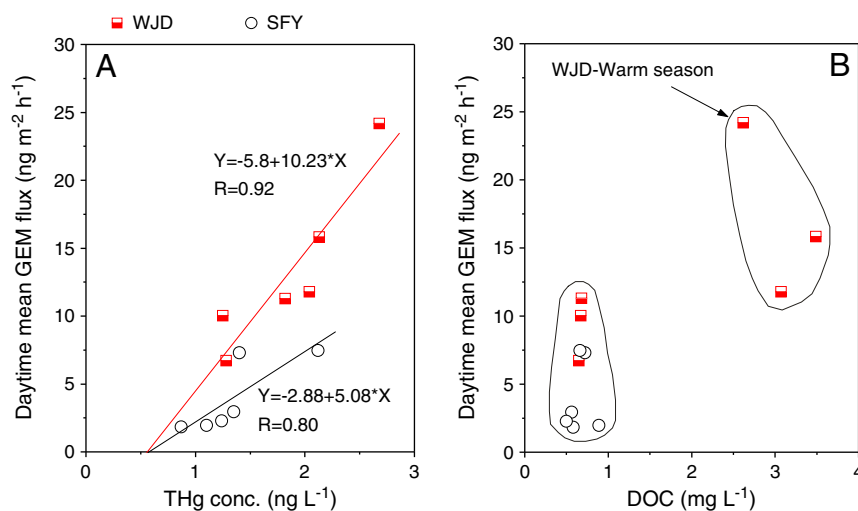

Fig. 5. Relationship analysis between daytime mean GEM fluxes and A) THg concentrations in surface water; and B) DOC concentrations in surface water.

Hence, the effect of DOC concentrations on GEM fluxes is still not very clear (Ravichandran, 2004). As indicated from Fig. 5B, the highest GEM fluxes were not related to the highest water DOC concentration. This might indicate that DOC has a complicated effect on GEM evasion fluxes, or it was caused by other mechanisms.

Moreover, microbial activities in the WJD reservoir might be also responsible for its high GEM evasion fluxes. Study by Poulain et al. (2004) suggested that photosynthesis of phytoplankton could generate reductants inside the cells and excrete reductants into the surrounding water, which could accelerate the production of DGM in fresh water. Also, plankton in surface water may adsorb Hg-dissolved organic matter compound and ultimately release GEM as a metabolic sub-product. It was reported that the abundance of phytoplankton in surface water of WJD ($\sim 9.2 \times 10^6$ cell L^{-1}) was much higher than that in SFY ($\sim 1.4 \times 10^6$ cell L^{-1}) (Yu, 2008). This was probably an important reason for elevated GEM evasion fluxes in WJD. Besides, the highly elevated nighttime GEM evasion fluxes in the warm season of WJD might also indicate the biological activities (Fig. 4).

Except for the above reasons, there should be other factors influencing the GEM fluxes in the two hyper-eutrophic reservoirs. For example, some studies (Zhang and Lindberg, 2001; Wollenberg and Peters, 2009) suggested that Fe(III) has a positive effect on the production of DGM and evasion fluxes. Also, sulfide complexes may also affect the transportation and speciation of Hg in freshwater environments (Wollenberg and Peters, 2009). Nevertheless, accelerated eutrophication of lakes and reservoirs is of particular concern in China. It was estimated that 37% of reservoirs, 41% of the large estuaries and 62% of major lakes in China have been eutrophic and or are eutrophying (Meng and Zhang, 2007; Wei and Liang, 2008; Liu et al., 2009). The eutrophication of reservoirs and lakes will probably accelerate Hg evasion from aquatic environments in China. Therefore, future studies with regard to the potential mechanism of eutrophication influencing water/air Hg flux are urgently needed.

3.5. Contribution of evasion flux to the Hg budget in WJD and SFY reservoirs

Previous studies in pristine lakes and open sea environments demonstrated that evasion of Hg contributed significantly to the loss of Hg from aquatic ecosystems (Gao et al., 2006; Sunderland and Mason, 2007; Selvendiran et al., 2009). Here, we also made a preliminary Hg mass balance study to evaluate the effects of evasion process on the fate and transport of Hg in the channel-type reservoirs in southwest China.

Meng et al. (2010) and Yao et al. (2010) reported that mean THg concentrations in water columns of WJD and SFY were 1.3 ± 0.56 and 1.2 ± 0.55 ng L^{-1}, respectively. Assuming that the water masses in WJD and SFY were 13.5×10^8 and 0.67×10^8 m^3, respectively, we estimate that the total mass of THg in WJD and SFY were 1750 ± 750 and 80 ± 37 g, respectively.

In this work, riverine input, runoff, wet and dry depositions are identified as sources of Hg to the reservoirs; whereas riverine outflow, water consumption for irrigation and industry, and evasion are major pathways for Hg output from reservoirs. Based on the monthly measurements of THg concentrations in streams flowing into or out WJD (mass-weighted concentration: $THg_{input} = 2.82 \pm 1.67$ ng L^{-1}, $THg_{output} = 2.62 \pm 0.49$ ng L^{-1}) and SFY (mass-weighted concentration: $THg_{input} = 2.34 \pm 0.46$ ng L^{-1}, $THg_{output} = 2.18 \pm 0.39$ ng L^{-1}) (Guo, 2008b), riverine input and output of Hg were estimated to be $18,100 \pm 10,700$ and $16,200 \pm 3030$ g in WJD and $13,100 \pm 2570$ and $11,700 \pm 2090$ g in SFY, respectively. Runoff inputs were estimated using the precipitation THg concentrations during rainy seasons and water masses of runoff (Guo et al., 2008a). The runoff inputs of Hg to WJD and SFY were 3640 ± 1370 and 1000 ± 540 g, respectively. Except for Hg concentrations originated from precipitation, Hg concentration in runoff also contains an important fraction of Hg that comes from the

leaching of soils and vegetations. Therefore, our estimations for runoff input were probably underestimated, and this should be more pronounced during heavy rain events which may contribute to a notable fraction. However, Hg in runoff is generally associated with particles, which may have a possibility to be deposited during transport in tributary streams. This could yield a decrease in runoff THg concentrations before flowing into the reservoirs. Therefore, the estimations of runoff THg inputs are subjected to many uncertainties.

Annual loadings of Hg to WJD and SFY via wet deposition were 1890 ± 1000 and 210 ± 120 g, respectively. The wet deposition flux in WJD was based on the measurements in the reservoir (Guo et al., 2008a). For SFY, measurement results at the dam of the Dongfeng reservoir (Guo et al., 2008a), which was the nearest sampling site to SFY, were taken into account for the estimation of wet deposition flux. Estimation of dry deposition to the reservoirs was accomplished using empirical models. Zheng (2006) reported that the mean RGM and PHg concentrations at a rural site in Wujiang River Basin were 90 ± 40 and 660 ± 800 pg m^{-3}, respectively. Dry deposition velocities for RGM and PHg to water were set at 2.0 and 0.29 cm s^{-1}, respectively (Lai et al., 2007). Thus, annual dry depositions of THg to WJD and SFY were calculated to be 5600 ± 4700 and 670 ± 600 g, respectively.

Evasion losses of Hg were estimated using the measurement results in this study. The mean GEM fluxes in WJD and SFY were 85.0 ± 56.4 and 18.8 ± 14.5 µg m^{-2} year^{-1}, respectively. Based on the fluxes and water areas, evasion of THg from WJD and SFY were estimated to be 4060 ± 2690 and 110 ± 80 g per year. As discussed in Sections 3.3 and 3.4, GEM fluxes in WJD and SFY reservoirs showed clear seasonal and spatial distributions. The relatively short samples period and limited sampling sites in this study may result in a large uncertainty in the estimation for evasion losses of THg.

It is a great challenge to make such an assessment of Hg mass balance in WJD and SFY because there are many uncertainties in the calculations. Hence the estimation made herein may be a qualitative assessment at best. Table 4 shows the summaries of THg mass, inputs and outputs in the two study reservoirs. In general, both WJD and SFY were net sinks of Hg. This is in a good agreement with previous mass studies (Gao et al., 2006; Feng et al., 2009; Jeremiason et al., 2009). Riverine input was the largest source, and water discharge for power generation was the largest output of Hg.

In general, Hg evasion constituted a limited contribution to the cycling of Hg in the two channel-type reservoirs. Loss of Hg via evasion from WJD and SFY reservoirs accounted for 17.5% and 0.8% of the total losses, which are much lower compared to the study result of a tropical reservoir in French Guiana (Muresan et al., 2007, 2008b). This is probably attributed to the extremely low reservoir surface area/drainage area ratio. However, it should be pointed out that the evasion of Hg might be likely an important mechanism for Hg losses

Table 4
Total mass, input and output inventories of THg in WJD and SFY reservoirs.

Reservoirs		WJD	SFY
Mean THg concentration in water column (ng L^{-1})		1.3 ± 0.56	1.2 ± 0.55
Total Hg mass (g)		1750 ± 750	80 ± 37
Input	Riverine input	$18,100 \pm 10,700$	$13,100 \pm 2570$
	Runoff input	3640 ± 1370	1000 ± 540
	Wet deposition	1890 ± 1000	210 ± 120
	Dry deposition	5600 ± 4700	670 ± 600
	Total input	$29,200 \pm 17,800$	$15,000 \pm 3830$
Output	Water discharge	$16,200 \pm 3030$	$11,700 \pm 2090$
	Evasion	4060 ± 2690	110 ± 80
	Others[a]	2870 ± 540	860 ± 150
	Total output	$23,100 \pm 6260$	$12,700 \pm 2320$
Sink		6100	2300

[a] Losses via water consumption for industrial use and agricultural irrigation (Guo, 2008b).

from other aquatic environments in China (e.g. lakes, ponds), which often have a larger water area/drainage area ratio compared to channel-type reservoirs. Besides, it is reported that many lakes in China experience the eutrophication problems (Meng and Zhang, 2007; Wei and Liang, 2008; Liu et al., 2009), which probably enhance the Hg evasion from water. Therefore, it is important and urgent to quantify this source category and further evaluate its effect on the biogeochemical cycling of Hg in aquatic environments in China.

4. Conclusion

Water/air GEM fluxes in two channel-type reservoirs in southwest China ranged from 0.6 to 20.1 ng m^{-2} h^{-1}, which were in a good agreement with previous measurements in southwest China but higher compared to the data observed in pristine lakes in North America. GEM fluxes exhibited a clear diurnal pattern with elevated evasion in the daytime and lower evasion or deposition during the night, and this trend was extremely pronounced in sunny days. Solar radiation was strongly correlated with the short-term fluctuation in GEM fluxes. Pronounced seasonal variation in GEM fluxes with highly elevated fluxes in warm seasons and lower fluxes in cold seasons was observed at all the sampling sites, which was probably attributed to the elevated water THg concentrations, solar radiation, air temperature, wind speed and water DOC content in the warm season. Interestingly, the evasion flux of Hg in WJD, a hyper-eutrophic reservoir, was much higher compared to SFY. Overall, it is speculated that the eutrophication played a significant role in the elevated GEM flux in WJD. The preliminary assessment of Hg mass balance in WJD and SFY reservoirs suggests that the most important mechanism for Hg losses from channel-type reservoirs was water discharge for power generation rather than volatilization.

Acknowledgement

References

Amyot M, Mierle G, Lean D, McQueen DJ. Effect of solar radiation on the formation of dissolved gaseous mercury in temperate lakes. Geochim Cosmochim Acta 1997;61: 975–87.
Boudala FS, Folkins I, Beauchamp S, Tordon R, Neima J, Johnson B. Mercury flux measurements over air and water in Kejimkujik National Park, Nova Scotia. Water Air Soil Pollut 2000;122:183–202.
Cao L, Wang WM, Yang Y, Yang CT, Yuan ZH, Xiong S, et al. Environmental impact of aquaculture and countermeasures to aquaculture pollution in China. Environ Sci Pollut Res 2007;14:452–62.
Coelho JP, Pereira ME, Duarte A, Pardal MA. Macroalgae response to a mercury contamination gradient in a temperate coastal lagoon (Ria de Aveiro, Portugal). Estuar Coast Shelf Sci 2005;65:492–500.
Cosovic B, Ciglenecki I, Vilicic D, Ahel M. Distribution and seasonal variability of organic matter in a small eutrophied salt lake. Estuar Coast Shelf S 2000;51:705–15.
Eggleton J, Thomas KV. A review of factors affecting the release and bioavailability of contaminants during sediment disturbance events. Environ Int 2004;30:973–80.
Feng XB, Qiu GL. Mercury pollution in Guizhou, Southwestern China — an overview. Sci Total Environ 2008b;400:227–37.
Feng X, Yan H, Wang S, Qiu G, Tang S, Shang L, et al. Seasonal variation of gaseous mercury exchange rate between air and water surface over Baihua reservoir, Guizhou, China. Atmos Environ 2004a;38:4721–32.
Feng X, Shang L, Wang S, Tang S, Zheng W. Temporal variation of total gaseous mercury in the air of Guiyang, China. J Geophys Res 2004b;109:D03303. doi:10.1029/2003JD004159.
Feng X, Wang S, Qiu G, He T, Li G, Li Z, et al. Total gaseous mercury exchange between water and air during cloudy weather conditions over Hongfeng Reservoir, Guizhou, China. J Geophys Res 2008a;113:D15309. doi:10.1029/2007JD009600.
Feng XB, Jiang HM, Qiu GL, Yan HY, Li GH, Li ZG. Mercury mass balance study in Wujiangdu and Dongfeng Reservoirs, Guizhou, China. Environ Pollut 2009;157: 2594–603.
Fu XW, Feng XB, Wang SF, Rothenberg S, Shang LH, Li ZG, Qiu GL. Temporal and spatial distributions of total gaseous mercury concentrations in ambient air in a mountainous area in southwestern China: implications for industrial and domestic mercury emissions in remote areas in China. Sci Total Environ 2009;42:970–9.

Fu XW, Feng XB, Dong ZQ, Yin RS, Wang JX, et al. Atmospheric gaseous elemental mercury (GEM) concentrations and mercury deposition at a high-altitude mountain peak in south China. Atmos Chem Phys 2010;10:2425–37.
Gao N, Armatas NG, Shanley JB, Kamman NC, Miller EK. Mass balance assessment for mercury in Lake Champlain. Environ Sci Technol 2006;40:82–9.
Garcia E, Laroulandie J, Saint-Simon XR, Amyot M. Temporal and spatial distribution and production of dissolved gaseous mercury in the Bay St. François wetland, in the St. Lawrence River, Quebec, Canada. Geochim Cosmochim Acta 2006;70:2665–78.
Gårdfeldt K, Feng XB, Sommar J, Lindqvist O. Total gaseous mercury exchange between air and water over lake and sea surfaces. Atmos Environ 2001;35:3027–38.
Guo YN. Input and output fluxes of mercury in different evolutive reservoirs in Wujiang River Basin. PH.D. dissertation, Graduate University of the Chinese Academy of Science, Bejing, China (in Chinese with abstract in English); 2008(b).
Guo YN, Feng XB, Li ZG, He TR, Yan HY, et al. Distribution and wet deposition fluxes of total and methyl mercury in Wujiang reservoir Basin, Guizhou, China. Atmos Environ 2008a;42:7096–103.
He T, Feng X, Guo Y, Qiu G, Li Z, Liang L, Lu J. The impact of eutrophication on the biogeochemical cycling of mercury species in a reservoir. A case study from Hongfeng Reservoir, Guizhou, China. Environ Pollut 2008;154:56–67.
Jeremiason JD, Kanne LA, Lacoe TA, Hulting M, Simcik MF. A comparison of mercury cycling in Lakes Michigan and Superior. J Great Lakes Res 2009;35:329–36.
Lai SO, Thomas SH, Han YJ, Hopke PP, Yi SM, et al. Estimation of mercury loadings to Lake Ontario: results from the Lake Ontario atmospheric deposition study (LOADS). Atmos Environ 2007;41:8205–18.
Lindberg SE, Meyers TP, Munthe J. Evasion of mercury vapor from the surface of a recently limed acid forest lake in Sweden. Water Air Soil Pollut 1995;85:725–30.
Lindberg SE, Zhang H, Vette AF, Gustin MS, Barnett MO, Kuiken T. Dynamic flux chamber measurement of gaseous mercury emission fluxes over soils. Part II: Effect of flushing flow rate and verification of a two-resistance exchange interface simulation model. Atmos Environ 2002;36:847–59.
Liu SM, Hong GH, Zhang J, Ye XW, Jiang XL. Nutrient budgets for large Chinese estuaries. Biogeosciences 2009;6:2245–63.
Mason RP, Sheu GR. Role of the ocean in the global mercury cycle. Global Biogeochem Cycles 2002;16(4):1093. doi:10.1029/2001GB001440.
Mason RP, Lawson NM, Lawrence AL, Leaner JJ, Lee JG, Sheu GR. Mercury in the Chesapeake Bay. Chemosphere 1999;65:77–96.
Meng HM, Zhang ZK. Actuality and assessment of primary reservoirs eutrophication in China. J Henan Normal Univ 2007;35:133–7 in Chinese with abstract in English.
Meng B, Feng XB, Chen CX, Qiu GL, Sommar J, Guo YN, et al. Influence of eutrophication on the distribution of total mercury and methylmercury in hydroelectric reservoirs. J Environ Qual 2010;39:1-12.
Muresan B, Cossa D, Coquery M, Richard S, Burban B. Mercury speciation and exchanges at the air-water interface of tropical artificial reservoir, French Guiana. Sci Total Environ 2007;253:132–45.
Muresan B, Cossa D, Coquery M, Richard S. Mercury sources and transformations in a man-perturbed tidal estuary: the Sinnamary Estuary, French Guiana. Geochim Cosmochim Acta 2008a;72:5416–30.
Muresan B, Cossa D, Richard S, Dominique Y. Monomethylmercury sources in a tropical artificial reservoir. Appl Geochem 2008b;23:1101–26.
O'Driscoll NJ, Poissant L, Canário J, Ridal J, Lean DRS. Continuous analysis of dissolved gaseous mercury and mercury volatilization in the upper St. Lawrence River; exploring temporal relationship and UV attenuation. Environ Sci Technol 2007;41:5342–8.
Peters SC, Wollenberg JL, Morris DP, Porter JA. Mercury emission to the atmosphere from experimental manipulation of DOC and UVR in mesoscale field chambers in a freshwater lake. Environ Sci Technol 2007;41:7356–62.
Pickhardt PC, Folt CL, Chen CY, Klaue B, Blum JD. Algal blooms reduce the uptake of toxic methylmercury in freshwater food webs. Proc Natl Acad Sci USA 2002;99(7):4419–23.
Poissant L, Casimir A. Water–air and soil–air exchange rate of total gaseous mercury measured at background sites. Atmos Environ 1998;32:883–93.
Poulain AJ, Amyot M, Findlay D, Telor S, Barkay T, Hintelmann H. Biological and photochemical production of dissolved gaseous mercury in a boreal lake. Limnol Oceanogr 2004;49:2265–75.
Qin BQ, Yang LY, Chen FZ, Zhu GW, Zhang L, Chen YY. Mechanism and control of lake eutrophication. Chin Sci Bull 2006;51:2401–12.
Radway JC, Wilde EW, Whitaker MJ, Weissman JC. Screening of algal strains for metal removal capabilities. J Appl Physiol 2001;13:451–5.
Ravichandran M. Interactions between mercury and dissolved organic matter—a review. Chemosphere 2004;55:319–33.
Schroeder WH, Beauchamp S, Edwards G, Poissant L, Rasmussen P, Tordon R, et al. Gaseous mercury emissions from natural sources in Canadian landscapes. J Geophys Res 2005;110:D18302. doi:10.1029/2004JD005699.
Selvendiran P, Driscoll CT, Montesdeoca MR, Choi HD, Holsen TM. Mercury dynamics and transport in two Adirondack lakes. Limnol Oceanogr 2009;54:413–27.
Strode SA, Jaeglé L, Selin NE, Jacob DG, Park RJ, Yantosca RM, et al. Air-sea exchange in the global mercury cycle. Global Biogeochem Cycles 2007;21:GB1017. doi: 10.1029/2006GB002766.
Sun JL, Zhong X, Liu YX, Fu J. The status analysis of cage culture fishing of reservoir and lake in Guizhou province. Guizhou Environ Prot Sci Technol 2005;11:30–4 in Chinese with abstract in English.
Sunderland EM, Mason RP. Human impacts on open ocean mercury concentrations. Global Biogeochem Cycles 2007;21:GB4022. doi:10.1029/2006GB002876.
Tseng CM, Lamborg C, Fitzgerald WF, Engstrom DR. Cycling of dissolved elemental mercury in Arctic Alaskan lakes. Geochim Cosmochim Acta 2004;68:1173–84.
US EPA. Method 1631: Revision B, Mercury in water by oxidation, purge and trap, and cold vapor atomic fluorescence spectrometry. United States Environmental Protection Agency; 1999. p. 1-33.

Wang DY, He L, Shi XJ, Wei SQ, Feng XB. Release flux of mercury from different environmental surfaces in Chongqing, China. Chemosphere 2006;64:1845–54.

Wang BL, Liu CQ, Wang FS, Yu YX, Zhang LH. The distributions of autumn picoplankton in relation to environmental factors in the reservoirs along the Wujiang River in Guizhou Province, SW China. Hydrobiologia 2008a;589:35–45.

Wang ZW, Zhang XS, Xiao JS, Ci ZJ, Yu PZ. Mercury fluxes and pools in three subtropical forested catchments, southwest China. Environ Pollut 2008b;157:801–8.

Wang BL, Liu CQ, Wang FS, Yu YX, Wu YY. Flow cytometric observation of picophytoplankton community structure in the cascade reservoirs along Wujiang River, SW China. J limnol 2009;68:53–63.

Wei LP, Liang MS. A summary of the problem of lake eutrophication in China. Chin Chem 2008;6:38–40 in Chinese with abstract in English.

Wollenberg JL, Peters SC. Mercury emission from a temperate lake during autumn turnover. Sci Total Environ 2009;407:2909–18.

Wu Y, Wang SX, Streets DG, Hao FM, Chan M, Jiang JK. Trends in anthropogenic mercury emissions in China from 1995 to 2003. Environ Sci Technol 2007;40:5312–8.

Xiao Z, Munthe J, Schroeder WH, Lindqvist O. Vertical fluxes of volatile mercury over forest soil and lake surfaces in Sweden. Tellus Ser B 1991;43:267–79.

Yan HY, Feng XB, Shang LH, Qiu GL, Dai QJ, Wang SF, et al. The variations of mercury in sediment profiles from a historically mercury-contaminated reservoir, Guizhou province, China. Sci Total Environ 2009;407:497–506.

Yao H, Feng XB. Distribution and speciation of mercury species in two newly constructed reservoirs within the WuJiang River, Guizhou Province, China. Environ Toxicol Chem 2010; in review.

Yu YX. The effects of cascaded damming on biogeochemical cycling of carbon in the middle-upper reaches of Wujiang River, SW China. PH.D. dissertation, Graduate University of the Chinese Academy of Science, Bejing, China (in Chinese with abstract in English);2008.

Zhang H, Lindberg SE. Sunlight and Fe(III)-induced photochemical production of dissolved gaseous mercury in freshwater. Environ Sci Technol 2001;35:928–35.

Zhang H, Lindberg SE, Barnett MO, Vette AF, Gustin MS. Dynamic flux chamber measurement of gaseous mercury emission fluxes over soils. Part I: Simulation of gaseous mercury emissions from soils using a two-resistance exchange interface model. Atmos Environ 2002;36:835–46.

Zhang HH, Poissant L, Xu XH, Pilote M, Beauvais C, Amyot M, et al. Air−water gas exchange of mercury in the Bay Saint Francois wetlands: observation and model parameterization. J Geophys Res 2006;111:D17307. doi:10.1029/2005JD006930.

Zheng W. Mercury species in the urban air of Guiyang. PH.D. dissertation, Graduate University of the Chinese Academy of Science, Bejing, China (in Chinese with abstract in English);2006.